



Cite this: *Chem. Commun.*, 2023, 59, 12128

Received 4th August 2023,  
Accepted 8th September 2023

DOI: 10.1039/d3cc03791f

rsc.li/chemcomm

# Fully tuneable ethylene–propylene elastomers using a supported permethylindenyl-phenoxy (PHENI\*) catalyst†

Clement G. Collins Rice,<sup>†</sup> Louis J. Morris,<sup>†</sup> Jean-Charles Buffet,<sup>†</sup>  
Zoë R. Turner<sup>†</sup> and Dermot O'Hare<sup>†</sup>\*

Using a highly active supported permethylindenyl-phenoxy (PHENI\*) titanium catalyst, high molecular weight ethylene–propylene (EPM) and ethylene–propylene–diene (EPDM) elastomers are prepared using slurry-phase catalysis. Final copolymer composition was found to reflect the monomer feed ratio in a linear fashion, to access a continuum of material properties with a single catalyst. Post-polymerisation crosslinking of EPDM was also demonstrated in a model sulfur vulcanisation system.

Conventional rubbers are highly crosslinked polymers which are challenging to process and have poor recyclability.<sup>1</sup> Thermoplastic elastomers (TPEs) are an emerging class of materials that bridge the gap between classical thermoset rubbers and thermoplastics, having the elastic properties of the former and the processing flexibility and recyclability of the latter.<sup>2,3</sup> This requires a biphasic structure with crystalline and amorphous regions. Block copolymers have proved promising with distinct hard and soft segments facilitating TPE behaviour.<sup>4–6</sup> Hyperbranched polyethylene has also been investigated as a direct route to the production of polyolefin elastomers.<sup>3,7</sup>

Copolymers of ethylene and propylene (EPM) are an important class of TPE, with extensive research relating the physical properties to the molecular weight, composition, and chain structure.<sup>8–10</sup> In particular, the crystalline microstructure of EPM has been shown to strongly influence yield stress and rupture energy density.<sup>9</sup> EPM displays homogeneous deformation, like most rubbers, but also yield-like behaviour more typical of thermoplastics. It has been shown that EPM composition controls not only crystallinity but also compatibility with polymer matrices,<sup>11</sup> polyolefin blends,<sup>12,13</sup> and recycled polyolefins.<sup>14</sup>

Vanadium-based catalysts dominate the industrial production of EPM,<sup>15</sup> though group four complexes have also been

studied,<sup>16</sup> with the Keltan ACE™ titanium  $\kappa^1$ -amidinate complexes being used to produce EPM commercially.<sup>17</sup> In general, the overwhelming preference for ethylene coordination-insertion relative to propylene ( $r_E \gg r_P$ ) leads to long sequences of consecutive ethylene units and this limits the compositional tunability that could potentially be possible to achieve.<sup>18–20</sup> The amidinate complexes produce EPM with 39–75 wt% ethylene from a feed containing 33% C<sub>2</sub> monomer.<sup>17,19</sup> A silica-supported zirconocene reported by Caballero *et al.* is a limited example of a catalyst able to produce EPM across the whole composition range by controlling the gas phase E:P ratio. Even in this case, a clear preference for ethylene is observed with 13% incorporated from a 3:97 E:P feed.<sup>10</sup>

Following our recent report of group four permethylindenyl-phenoxy (PHENI\*) catalysts, and their outstanding performance for ethylene and propylene homopolymerisation,<sup>21,22</sup> we now describe the application of the PHENI\* complex  $\text{Me}_2\text{SB}(\text{Bu}_2\text{ArO}, \text{I}^*)\text{TiCl}_2$  ( $\{(\eta^5\text{-C}_9\text{Me}_6)\text{Me}_2\text{Si}(2,4\text{-tBu}_2\text{-C}_6\text{H}_2\text{O})\}\text{TiCl}_2$ ), heterogenised on solid polymethylaluminoxane (sMAO),<sup>23</sup> **1** (Fig. 1), for the production of EPM elastomers. sMAO is well-established as a dual function activating support for metallocene and post-metallocene catalysts.<sup>24,25</sup> The catalyst system displays an unusual monomer-agnostic behaviour resulting in access to fully tuneable compositions of high molecular weight EPM.

The sMAO-supported PHENI\* complex  $\text{sMAO}\text{-Me}_2\text{SB}(\text{Bu}_2\text{ArO}, \text{I}^*)\text{TiCl}_2$  ( $[\text{Al}_{\text{sMAO}}]_0/[\text{Ti}]_0 = 200$ ; **1**) was prepared,<sup>21,22</sup> and utilised in slurry-phase olefin copolymerisations. Polymerisations were carried out within a temperature of polymerisation ( $T_p$ )

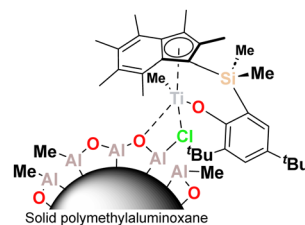


Fig. 1 Schematic structure of sMAO-supported PHENI\* catalyst **1**.

Chemistry Research Laboratory, Department of Chemistry, University of Oxford,  
12 Mansfield Road, Oxford, OX1 3TA, UK. E-mail: dermot.ohare@chem.ox.ac.uk

† Electronic supplementary information (ESI) available: Experimental procedures, polymerisation data, polymer characterisation data. Copolymerisation of propylene and 1-hexene is discussed in the ESI. See DOI: <https://doi.org/10.1039/d3cc03791f>



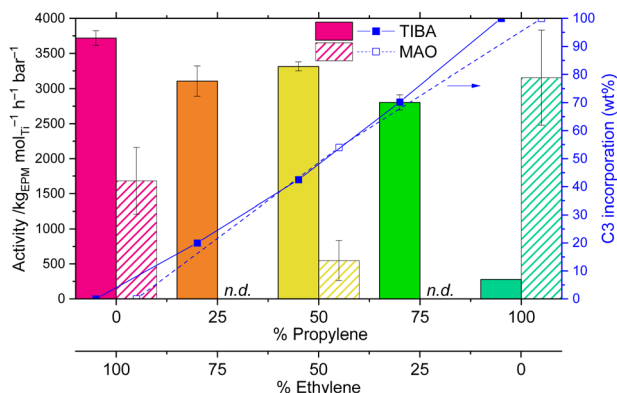


Fig. 2 Mean polymerisation activity and propylene incorporation as a function of monomer feed composition for 1/TIBA and 1/MAO. Polymerisation conditions: 10 mg **1**, 2 bar total pressure, 50 mL hexanes, either 150 mg TIBA or MAO ( $[Al]_0/[Ti]_0 = 1000$ ), 60 °C, and 30 minutes. Incorporation determined by GPC-IR. Error bars shown at one standard deviation. *n.d.* indicates no data.

range of  $30 \leq T_p \leq 90$  °C under 2 bar total pressure with 10 mg of **1** ( $\sim 712$  nmol Ti) and either MAO or TIBA as cocatalyst ( $[Al]_0/[Ti]_0 = 1000$ ) in 50 mL hexanes as a diluent.

In the homopolymerisation of ethylene, 1/TIBA showed the greatest catalytic activity, while for homopolypropylene the highest activities were achieved with 1/MAO (Fig. 2). Therefore, E/P copolymerisations were performed using a 50:50 monomer feed mixture and either MAO or TIBA. In this case, 1/TIBA displayed significantly higher copolymerisation activity than 1/MAO: 3313 and 548 kg<sub>EPM</sub> mol<sub>Ti</sub><sup>-1</sup> h<sup>-1</sup> bar<sup>-1</sup> respectively. It has previously been noted that TIBA can transalkylate with MAO, leading to *iso*-butyl substituted aluminoxanes that are almost inactive towards propylene polymerisation.<sup>26</sup> When using 1/TIBA, E/P copolymerisation activity was comparable to that of ethylene homopolymerisation (3719 kg<sub>PE</sub> mol<sub>Ti</sub><sup>-1</sup> h<sup>-1</sup> bar<sup>-1</sup>), though in a highly dissimilar diffusion regime: while polyethylene was formed as well dispersed solid particles,<sup>21</sup> EPM is hexane-soluble at all compositions studied, and forms as a gel. Copolymerisations were subsequently run using E:P ratios of 25:75 and 75:25 with 1/TIBA as the catalyst system (Fig. 2). In these cases, activity is approximately independent of monomer feed composition, being within 1 standard deviation of each other.

Copolymer composition demonstrated precise tuneability, with the monomer ratio in the EPM corresponding almost exactly to that in the feed gas mixture. By GPC-IR, the EPM copolymers were found to contain 20, 42, and 71 wt% propylene (Fig. 2) from E/P feeds of 75:25, 50:50, and 25:75 respectively; this was confirmed by quantitative solution-phase <sup>13</sup>C{<sup>1</sup>H} NMR spectroscopy, which gave values of 16, 50, and 75 mol% propylene. Remarkably, the polymer composition was not found to significantly depend on the temperature of polymerisation ( $30 \leq T_p \leq 90$  °C), being in the range 40–47 wt% propylene incorporation when 50:50 E:P feed gas was utilised (Fig. S3 and S4, ESI†). Such direct tuneability of the comonomer composition as an almost 1-to-1 function of the feed gas is an unusual feature of the PHENI\* catalyst system.

By contrast, the [O-NS] titanium complex used by Yao *et al.* produced EPM with up to 29.5 mol% propylene incorporation at 60 °C, even when the feed was 33:67 E:P. Whilst the incorporation was approximately linear over the composition regimes studies in that case, it was far from a 1-to-1 relationship.<sup>20</sup> The commercial Keltan ACE™ complexes have demonstrated activities as high as 133 750 kg<sub>EPM</sub> mol<sub>Ti</sub><sup>-1</sup> h<sup>-1</sup> bar<sup>-1</sup> and molecular weights of 1.3–1.7 MDa. In general, though, these  $\kappa^1$ -amidinate complexes preferentially incorporate ethylene, with just one example of an EPM, having 61 wt% P, approaching the composition of the feed (33:67 E:P).<sup>17</sup> Vanadium compounds dominate the commercial production of ethylene-propylene copolymers. The vanadium(III) NHC complexes reported by Zhang *et al.* were able to incorporate up to 39 mol% propylene under a 75:25 E:P monomer supply.<sup>27</sup> Caballero *et al.* used the catalyst  $\{(\eta^5\text{-2-Me-C}_9\text{H}_5)_2\text{SiMe}_2\}\text{ZrCl}_2$  to synthesise a complete range of EPM compositions, though the system preferentially polymerised ethylene, with a 3:97 E:P feed resulting in a polymer with 13 mol% ethylene.<sup>10</sup> The titanium half-sandwich complexes reported by Zhang *et al.*, which use X-type anionic nitrogen-based donors, demonstrated activities of up to 2390 kg<sub>EPM</sub> mol<sub>Ti</sub><sup>-1</sup> h<sup>-1</sup>.<sup>19</sup> In this case, an E:P ratio of 33:67 resulted in 38 mol% propylene incorporation, and a viscosity-average molecular weight,  $M_{\eta}$ , of 340 kDa. The activity of PHENI\* compares favourably to this as well as offering full compositional tunability.

The resulting EPM produced by 1/TIBA was found to be amorphous by DSC, consistent with the formation of a random copolymer. Polymer molecular weight and distribution were estimated from GPC as well as short-chain branching (SCB) density and composition from an inline IR detector. Weight-average molecular weight ( $M_w$ ) of EPM (E:P 50:50) was found to be greater when the scavenger was MAO rather than TIBA, 290 and 150 kDa respectively, due to a high molecular weight shoulder in the chromatogram. This is reflected in a greater dispersity ( $\bar{D}$ ) of 3.1 when using MAO compared to 2.3 with TIBA, close to the ideal value for single-site polymerisation. Both  $M_w$  and  $\bar{D}$  were largely independent of feed composition, with  $M_w$  in the range 150–160 kDa from 25–75% propylene.

Engineering stress-strain curves were obtained for vacuum compression moulded samples of EPM (Fig. 3). Compared to HDPE of comparable  $M_w$ , the EPM synthesised with 75:25 E:P shows a much greater strain at break ( $\epsilon_B = 974\%$  *cf.* 170%) afforded by the elastomeric properties of *a*PP segments. Strain hardening is observed after a yield-like point at  $\epsilon_y = 60\%$  associated with the crystalline behaviour of the polyethylene segments. By contrast, at higher propylene incorporations the EPM displays poor mechanical performance with decreased strength and  $\epsilon_B$ . In these cases the amorphous nature of the *a*PP segments is responsible for the degraded behaviour, while the  $M_w$  is insufficient to achieve the desirable elastic properties of UHMW $\alpha$ PP.<sup>22</sup>

Following the successful synthesis of EPM polymers at high activity and with tuneable composition, 1/TIBA was used in the terpolymerisation of ethylene, propylene, and 5-ethylidene-2-norbornene (ENB). As well as being easier to handle than



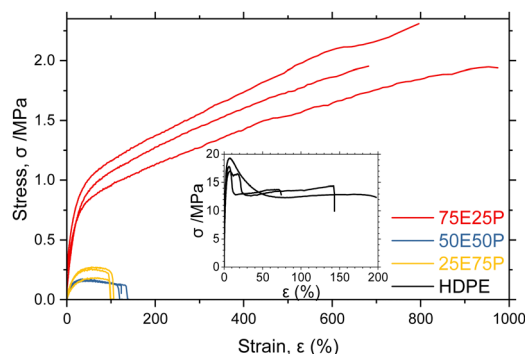


**Fig. 3** Engineering stress–strain curves of EPM as a function of composition. Inset: Engineering stress–strain curve of a commercial HDPE ( $M_w = 225$  kDa,  $D = 25$ ).

butadiene, ENB is commonly used as a diene in multicomponent polymerisations. Only the internal norbornyl olefin participates in polymerisation, with the ethylidene providing pendant unsaturation to the polymer backbone for post-synthesis vulcanisation such as using UV light, sulfur (Scheme 1), or organic peroxides.<sup>28–31</sup> Excellent physical and mechanical properties, including resistance to ozone, heat, chlorine, oxygen, and weathering, make EPDM the most suitable rubbers for outdoor applications, tubing, insulating materials, and automotive applications.<sup>32</sup>

Under a 50:50 E:P feed (2 bar), after initially increasing by 56% to  $5155 \text{ kg}_{\text{EPDM}} \text{ mol}^{-1} \text{ h}^{-1} \text{ bar}^{-1}$  at  $78 \mu\text{L}$  ENB (12 mM) relative to homopolymerisation, terpolymerisation activity decreased as [ENB] increased (Fig. 4), reaching  $1065 \text{ kg}_{\text{EPDM}} \text{ mol}^{-1} \text{ h}^{-1} \text{ bar}^{-1}$  at  $625 \mu\text{L}$  (93 mM).  $M_w$  increased slightly with increasing ENB loading, reaching 204 kDa at  $625 \mu\text{L}$ , 36% higher than the E:P copolymerisation in the absence of ENB, resulting from poor chain transfer to ENB.<sup>34</sup>

The composition of the EPDM polymers was determined by solution-phase  $^1\text{H}$  NMR spectroscopy, according to the assignments and integral analysis of Leone *et al.*<sup>35</sup> The proportion of ENB in the terpolymer increases with increasing [ENB] from 1.8 mol% at  $78 \mu\text{L}$  (12 mM) to 13.4 mol% at  $625 \mu\text{L}$  (93 mM) (Fig. 4). The complex (EBI)ZrCl<sub>2</sub> studied by Ali *et al.* produced EPDM with composition 79.5:18.2:2.30 mol% (E:P:ENB) from an 80:20 E:P feed with 60 mM ENB at an activity of  $3.55 \times 10^6 \text{ kg}_{\text{EPDM}} \text{ mol}^{-1} \text{ h}^{-1}$ .<sup>34</sup> Malmberg *et al.* used the same catalyst and achieved ENB incorporations of up to 16 mol%

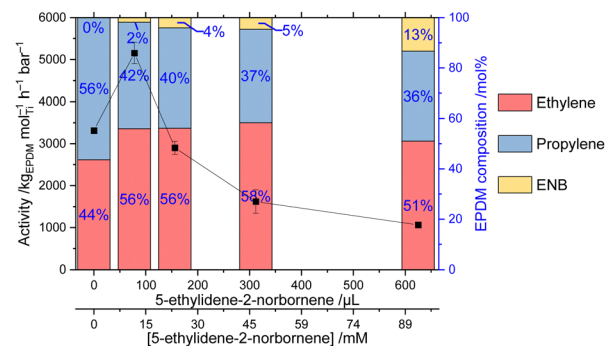
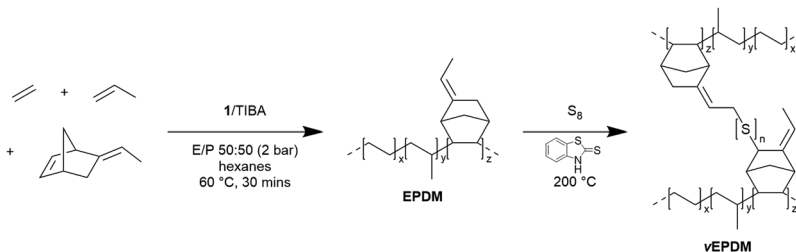


**Fig. 4** Mean terpolymerisation activity of **1**/TIBA and EPDM composition as a function of ENB loading ( $0 \leq V \leq 625 \mu\text{L}$ ;  $0 \leq c \leq 93$  mM). Composition determined from  $^1\text{H}$  NMR spectroscopy. Polymerisation conditions: 10 mg **1**, 2 bar ethylene/propylene (50:50), 50 mL hexanes, 150 mg TIBA,  $60^\circ\text{C}$ , and 30 minutes. Error bars shown at one standard deviation.

at a 600 mM concentration.<sup>36</sup> The vanadium(v) complexes studied by Leone *et al.* produced polymer with composition 80.3:6.5:13.2 mol% from an 18:73:9 feed at an activity of  $3006 \text{ kg}_{\text{EPDM}} \text{ mol}^{-1} \text{ h}^{-1}$ .<sup>35</sup> Compared to these complexes, the PHENI\* catalyst enchains ENB more efficiently, with higher incorporation at smaller concentrations, and produces EPDM with a composition that more closely matches the monomer feed.

A system comprising sulfur and the common accelerant 2-mercaptobenzothiazole ( $\text{C}_6\text{H}_4(\text{NH})\text{SC}=\text{S}$ , MBT) was used to vulcanise the as produced EPDM.<sup>33,37–42</sup> Relatively high loadings of  $\text{S}_8$  (10 phr; parts per hundred rubber) and MBT (5 phr) were used to ensure, in the absence of optimisations, sufficiently high conversion of ENB residues. Vulcanisations were performed in  $50 \mu\text{L}$  DSC pans, and the reactions were followed by dynamic DSC protocols established by Restrepo-Zapata *et al.*<sup>41</sup> The thermograms show endothermic features corresponding to the melting points of sulphur ( $113^\circ\text{C}$ ) and MBT ( $177\text{--}181^\circ\text{C}$ ), and an exotherm between  $180\text{--}230^\circ\text{C}$ , which is indicative of curing occurring by sulfur crosslinking (Fig. S6, ESI†). Furthermore, the vulcanisation was followed by dynamic rheology (Fig. S7, ESI†). During the initial temperature ramp the onset of crosslinking was observed at  $175^\circ\text{C}$  corresponding to a maximum in  $\tan(\delta)$ , with the storage modulus,  $G'$ , increasing rapidly as the reaction progresses from a starting value of 25 kPa to a final value of 1.1 MPa after 140 minutes of curing at



**Scheme 1** E/P/ENB terpolymerisation, and subsequent sulfur vulcanisation to form vEPDM, the structure of which is adapted from the mechanism provided by Verbruggen *et al.*<sup>33</sup>

200 °C. The storage modulus is associated with the elastic response of a viscoelastic material and so the observed increase corresponds to the presence of crosslinks which are able to store elastic potential energy.

In the infrared spectrum of the resulting vulcanised material (vEPDM) additional transitions are observed compared to EPDM arising from C–H and C–C vibrations corresponding to the crosslinks,<sup>43</sup> and C–S vibrations are seen in the region 775–600 cm<sup>−1</sup> (Fig. S8, ESI†).<sup>44</sup> The solid-state <sup>13</sup>C CPMAS NMR spectrum of vEPDM shows a broad resonance around 110–155 ppm, not present in the solution-phase spectrum of EPDM, and which corresponds to C–S resonances at the crosslink junctions  $\alpha$  to the pendant olefin. Winters *et al.* showed that broad resonances in ssNMR spectra at  $\delta$  117 and 151 ppm arise from EPDM vulcanisation.<sup>38</sup>

In conclusion, the PHENI\* catalyst has demonstrated excellent catalytic performance towards ethylene–propylene copolymerisations. The synthesis of EPM and EPDM is reported with high activities, high molecular weights, and fully tuneable composition. In all cases, composition can be controlled and tuned by the ratio of monomers in the feed, highlighting the desirable and unusually monomer-agnostic behaviour of this catalyst. The versatility of this chemistry has been demonstrated by the terpolymerisation with a diene and the latent unsaturation undergoing post-polymerisation crosslinking.

C. G. C. R., L. J. M., J.-C. B., and Z. R. T. would like to thank SCG Chemicals PLC for financial support. C. G. C. R. additionally acknowledges funding from the Engineering and Physical Sciences Research Council IAA (EP/X525777/1). The authors thank Ms Liv Thobru, Ms Sara Rund Herum, and Ms Rita Jenssen (Norner AS, Norway) for GPC analysis.

## Conflicts of interest

There are no conflicts of interest to declare.

## Notes and references

- 1 A. A. Yehia, *Polym. Plast. Technol. Eng.*, 2004, **43**, 1735–1754.
- 2 A. S. Mohite, Y. D. Rajpurkar and A. P. More, *Polym. Bull.*, 2022, **79**, 1309–1343.
- 3 K. Lian, Y. Zhu, W. Li, S. Dai and C. Chen, *Macromolecules*, 2017, **50**, 6074–6080.
- 4 K. S. O'Connor, A. Watts, T. Vaidya, A. M. LaPointe, M. A. Hillmyer and G. W. Coates, *Macromolecules*, 2016, **49**, 6743–6751.
- 5 C. M. Koo, M. A. Hillmyer and F. S. Bates, *Macromolecules*, 2006, **39**, 667–677.
- 6 Y. Zhao, Y. Ma, Y. Xiong, T. Qin, Y. Zhu, H. Deng, J. Qin, X. Shi and G. Zhang, *Polymer*, 2022, **254**, 125075.
- 7 Q. Mahmood and W.-H. Sun, *R. Soc. Open Sci.*, 2018, **5**, 180367.
- 8 W. J. Wang and S. Zhu, *Macromolecules*, 2000, **33**, 1157–1162.
- 9 K. J. Wright and A. J. Lesser, *Macromolecules*, 2001, **34**, 3626–3633.
- 10 M. J. Caballero, I. Suarez, B. Coto, R. Van Grieken and B. Monrabal, *Macromol. Symp.*, 2007, **257**, 122–130.
- 11 P. Doshev, G. Lohse, S. Henning, M. Krumova, A. Heuvelsland, G. Michler and H.-J. Radusch, *J. Appl. Polym. Sci.*, 2006, **101**, 2825–2837.
- 12 L. D'Orazio, R. Greco, C. Mancarella, E. Martuscelli, G. Ragosta and C. Silvestre, *Polym. Eng. Sci.*, 1982, **22**, 536–544.
- 13 S. Jose, S. Thomas, P. K. Biju and J. Karger-Kocsis, *J. Polym. Res.*, 2013, **20**, 303.
- 14 G. Radonjić and N. Gubelj, *Macromol. Mater. Eng.*, 2002, **287**, 122–132.
- 15 A. M. F. Phillips, H. Suo, M. D. F. C. Guedes da Silva, A. J. L. Pombeiro and W. H. Sun, *Coord. Chem. Rev.*, 2020, **416**, 213332.
- 16 R. Kravchenko and R. M. Waymouth, *Macromolecules*, 1998, **31**, 1–6.
- 17 G. van Doremale, M. van Duin, M. Valla and A. Berthoud, *J. Polym. Sci., Part A: Polym. Chem.*, 2017, **55**, 2877–2891.
- 18 C. Cozewith and G. V. Strate, *Macromolecules*, 1971, **4**, 482–489.
- 19 Z. Q. Zhang, J. T. Qu, S. Zhang, Q. P. Miao and Y. X. Wu, *Polym. Chem.*, 2018, **9**, 48–59.
- 20 Z. Yao, D. F. Ma, Z. X. Xiao, W. L. Yang, Y. X. Tu and K. Cao, *RSC Adv.*, 2017, **7**, 10175–10182.
- 21 C. G. Collins Rice, J.-C. Buffet, Z. R. Turner and D. O'Hare, *Chem. Commun.*, 2021, **57**, 8600–8603.
- 22 C. G. Collins Rice, J.-C. Buffet, Z. R. Turner and D. O'Hare, *Polym. Chem.*, 2022, **13**, 5597–5603.
- 23 T. J. Williams, J. V. Lamb, J.-C. Buffet, T. Khamnaen and D. O'Hare, *RSC Adv.*, 2021, **11**, 5644–5650.
- 24 A. F. R. Kilpatrick, J.-C. Buffet, P. Nørby, N. H. Rees, N. P. Funnell, S. Sripathongnak and D. O'Hare, *Chem. Mater.*, 2016, **28**, 7444–7450.
- 25 E. Kaji and E. Yoshioka, US8404880B2, 2013.
- 26 H. Kurokawa and T. Sugano, *Macromol. Symp.*, 1995, **97**, 143–149.
- 27 S. Zhang, W. C. Zhang, D. D. Shang and Y. X. Wu, *J. Polym. Sci., Part A: Polym. Chem.*, 2019, **57**, 553–561.
- 28 W. Wang and B. Qu, *Polym. Degrad. Stab.*, 2003, **81**, 531–537.
- 29 G. Milani and F. Milani, *J. Appl. Polym. Sci.*, 2012, **124**, 311–324.
- 30 E. A. Snijders, A. Boersma, B. Van Baarle and P. Gijsman, *Polym. Degrad. Stab.*, 2005, **89**, 484–491.
- 31 M. Van Duin, R. Orza, R. Peters and V. Chechik, *Macromol. Symp.*, 2010, **291**, 66–74.
- 32 I. Surya, M. Muniyandi and H. Ismail, *Polym. Compos.*, 2021, **42**, 1698–1711.
- 33 M. A. L. Verbruggen, L. van der Does, J. W. M. Noordermeer and M. van Duin, *J. Appl. Polym. Sci.*, 2008, **109**, 976–986.
- 34 A. Ali, M. K. Tufail, M. I. Jamil, W. Yaseen, N. Iqbal, M. Hussain, A. Ali, T. Aziz, Z. Fan and L. Guo, *Molecules*, 2021, **26**, 2037.
- 35 G. Leone, G. Zanchin, R. Di Girolamo, F. De Stefano, C. Lorber, C. De Rosa, G. Ricci and F. Bertini, *Macromolecules*, 2020, **53**, 5881–5894.
- 36 A. Malmberg and B. Löfgren, *J. Appl. Polym. Sci.*, 1997, **66**, 35–44.
- 37 S. Cesca, *J. Polym. Sci., Part D: Macromol. Rev.*, 1975, **10**, 1–230.
- 38 R. Winters, W. Heinen, M. A. L. Verbruggen, J. Lugtenburg, M. van Duin and H. J. M. de Groot, *Macromolecules*, 2002, **35**, 1958–1966.
- 39 M. Mortazavi, H. Arabi, S. Ahmadjo, M. Nekoomanesh and G. H. Zohuri, *J. Appl. Polym. Sci.*, 2011, **122**, 1838–1846.
- 40 N. Sanches, S. Cassu, M. Diniz and R. Lazzarini Dutra, *Polimeros*, 2014, **24**, 269–275.
- 41 N. C. Restrepo-Zapata, T. A. Osswald and J. P. Hernández-Ortiz, *Polym. Eng. Sci.*, 2015, **55**, 2073–2088.
- 42 D. Z. Pirityi and K. Pölöskei, *Polymers*, 2021, **13**, 1116.
- 43 F. J. Linnig and J. E. Stewart, *Rubber Chem. Technol.*, 1958, **31**, 719–736.
- 44 G. Socrates, *Infrared and Raman Characteristic Group Frequencies*, John Wiley & Sons Ltd, 3rd edn, 2004.

